The Ino80 chromatin-remodeling complex restores chromatin structure during UV DNA damage repair

Sovan Sarkar, Rhian Kiely, and Peter J. McHugh

Weatherall Institute of Molecular Medicine, University of Oxford, John Radcliffe Hospital, Oxford OX3 9DS, England, UK

Chromatin structure is modulated during deoxyribonucleic acid excision repair, but how this is achieved is unclear. Loss of the yeast Ino80 chromatin-remodeling complex (Ino80-C) moderately sensitizes cells to ultraviolet (UV) light. In this paper, we show that *INO80* acts in the same genetic pathway as nucleotide excision repair (NER) and that the Ino80-C contributes to efficient UV photoproduct removal in a region of high nucleosome occupancy. Moreover, Ino80 interacts with the early NER damage recognition complex Rad4–Rad23 and is recruited to chromatin by Rad4 in a UV damage–dependent manner. Using a modified chromatin immunoprecipitation assay, we find that chromatin disruption during UV lesion repair is normal, whereas the restoration of nucleosome structure is defective in *ino80* mutant cells. Collectively, our work suggests that Ino80 is recruited to sites of UV lesion repair through interactions with the NER apparatus and is required for the restoration of chromatin structure after repair.

Introduction

DNA lesions that induce helical distortion are repaired by the versatile nucleotide excision repair (NER) apparatus, which has been well characterized through biochemical reconstitution studies (Aboussekhra et al., 1995; Guzder et al., 1995; Mu et al., 1995; Riedl et al., 2003; Staresincic et al., 2009). Knowledge of how NER occurs in the complex chromatin environment of the nucleus is limited. Chromatin is disrupted to permit efficient NER, and chromatin structure is restored after repair (the access–repair–restore model; Smerdon, 1991; Green and Almouzni, 2002; Dinant et al., 2008). Histone chaperones (Caf1 and Asf1) are required for the restoration of chromatin structure after NER (Mello et al., 2002; Polo et al., 2006). Less is known about how chromatin access is achieved during NER. Human switch/sugar nonfermentable and *Drosophila melanogaster* ATPase-remodeling factors stimulate NER reactions performed in vitro on nucleosomal templates (Ura et al., 2001; Hara and Sancar, 2003). The yeast Snf5/6-remodeling proteins contribute to efficient cellular NER (Gong et al., 2006), and histone acetyltransferases modulate in vivo rates of NER at certain genomic locations (Teng et al., 2008). Finally, ubiquitination of the histones H3 and H4 by the CUL4–DDB1–ROC1 complex regulates the recruitment of xeroderma pigmentosum group C to DNA damage in mammalian cells (Wang et al., 2006).

Chromatin remodeling during DNA double-strand break (DSB) repair has been reviewed in detail previously (for reviews see Downs et al., 2007; Osley et al., 2007; van Attikum and Gasser, 2009), and we will briefly summarize this work, focusing on the Ino80 chromatin-remodeling complex (Ino80-C). The Ino80-C is an ATPase capable of nucleosome sliding in vitro (Shen et al., 2000) and is recruited to the DSBs in a γ-H2A–dependent fashion, perhaps via its Arp4 and Nhp10 subunits (Downs et al., 2004; Morrison et al., 2004; van Attikum et al., 2004). The Ino80-C might displace nucleosomes in the vicinity of a DSB (Tsukuda et al., 2005; van Attikum et al., 2007; Chen et al., 2008), and Arp8 (a subunit of the Ino80-C) has been shown to influence the rate of loading of Rad51 at breaks, possibly through a role in nucleosome displacement, independent of H2A phosphorylation (Tsukuda et al., 2005). Most recently, several groups have implicated the Ino80-C in replication restart after replicative stress and in damage tolerance pathways during replication (Papamichos-Chronakis

S. Sarkar and R. Kiely contributed equally to this paper.

Correspondence to Peter J. McHugh: peter.mchugh@imm.ox.ac.uk

R. Kiely's present address is Dept. of Biochemistry, University of Oxford, Oxford OX1 3QU, England, UK.

Abbreviations used in this paper: ChIP, chromatin immunoprecipitation; CPD, cyclobutane pyrimidine dimer; DSB, double-strand break; Ino80-C, Ino80 chromatin-remodeling complex; NER, nucleotide excision repair.

The Rockefeller University Press $30.00
J. Cell Biol. Vol. 191 No. 6 1061–1068
www.jcb.org/cgi/doi/10.1083/jcb.201006178

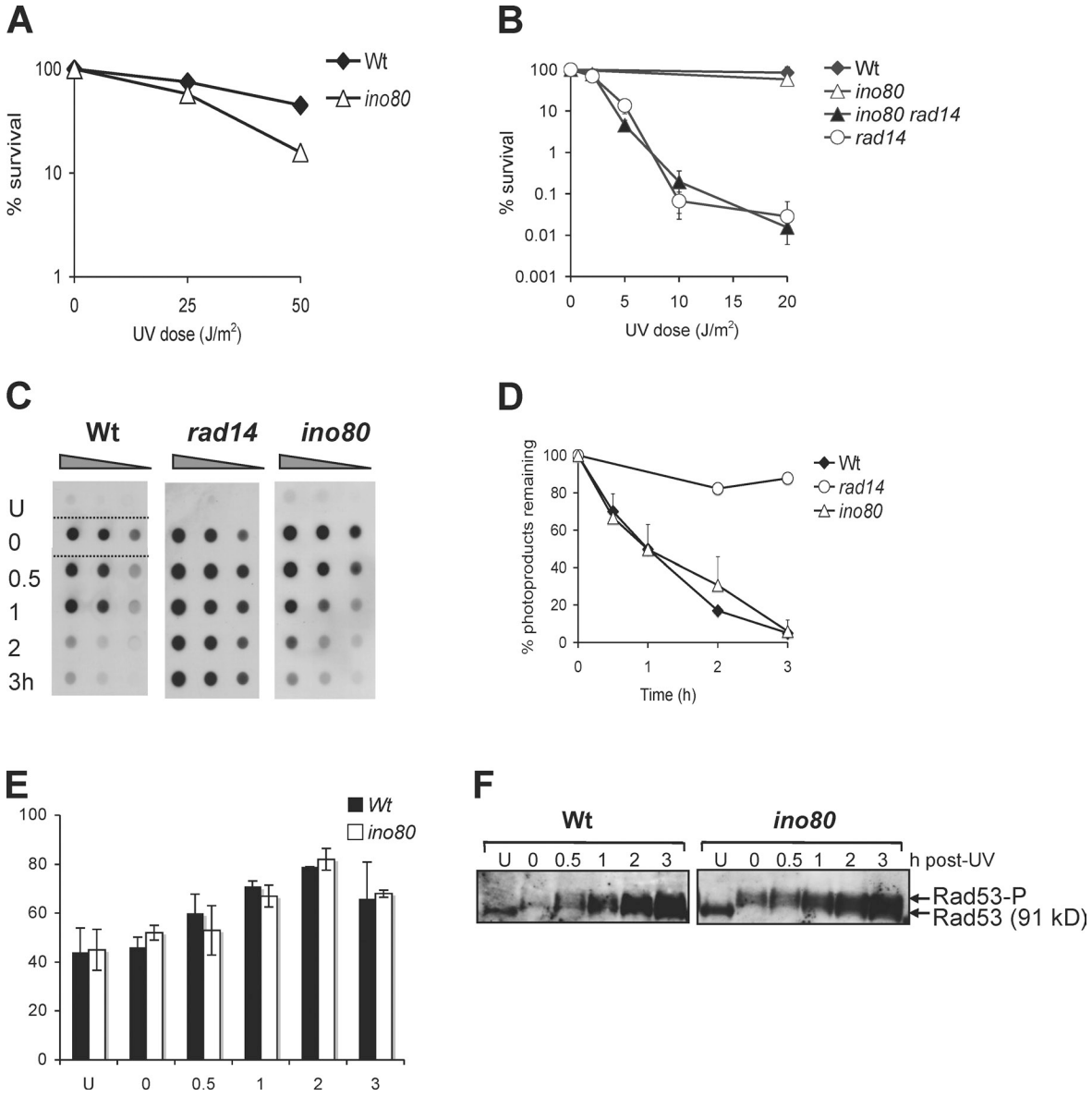

Figure 1. ***ino80* cells are UV sensitive but not defective in global photoproduct removal.** (A) Survival of *ino80* and wild-type (Wt) cells after exposure to UVC. (B) Survival of *rad14*, *ino80*, and *ino80 rad14* disruptants after exposure to UVC. (C) Dot blot analysis of CPD removal from genomic DNA in wild-type, *rad14*, and *ino80* strains after 50 J/m^2 UVC. The tapered symbols indicate serial (doubling) dilutions in DNA loading. The dashed lines indicate where a lane was spliced out. (D) Quantification of the blots shown in C. (E) Accumulation of large-budded cells after 100 J/m^2 UV irradiation in wild-type and *ino80* cells. All results are the means of three experiments, and error bars show the standard error of the mean. (F) Induction of phosphorylated Rad53 (Rad53-P) in wild-type and *ino80* cells after 100 J/m^2 UV irradiation. U, mock-treated cells.

and Peterson, 2008; Shimada et al., 2008; Falbo et al., 2009). Here, we report a role for the Ino80-C during chromatin restoration associated with UV lesion repair in yeast.

Results and discussion

Cells lacking Ino80 are UV sensitive but globally repair photoproducts normally

Formal killing curves confirmed a moderate UV sensitivity for *ino80* cells, as previously reported (Fig. 1 A; Shen et al., 2000). A strain co-deleted for *ino80* and *rad14* was no more sensitive than the *rad14* strain, suggesting that *ino80* is epistatic to NER factors (survival of *ino80* single disruptant at 20 J/m^2 = 54% and survival of the wild-type strain at 20 J/m^2 = 84%; Fig. 1 B). Dot blot assays were used to monitor the removal of UV photoproducts from cellular DNA. A wild-type strain removes cyclobutane pyrimidine dimers (CPDs) almost completely over 3 h (Fig. 1, C and D). A *rad14* NER mutant was, as expected, completely defective in this process. Quantification of the blots for *ino80* cells revealed no significant defect in the removal of CPDs (Fig. 1 D), and consistent results were obtained by probing with an anti–6-4 photoproduct antibody (not depicted). Therefore, despite being UV sensitive and epistatic to *rad14*, *ino80* mutants have no major global defect in the removal of UV photoproducts.

The UV sensitivity of *ino80* strains might be caused by a checkpoint defect. Therefore, we monitored the accumulation

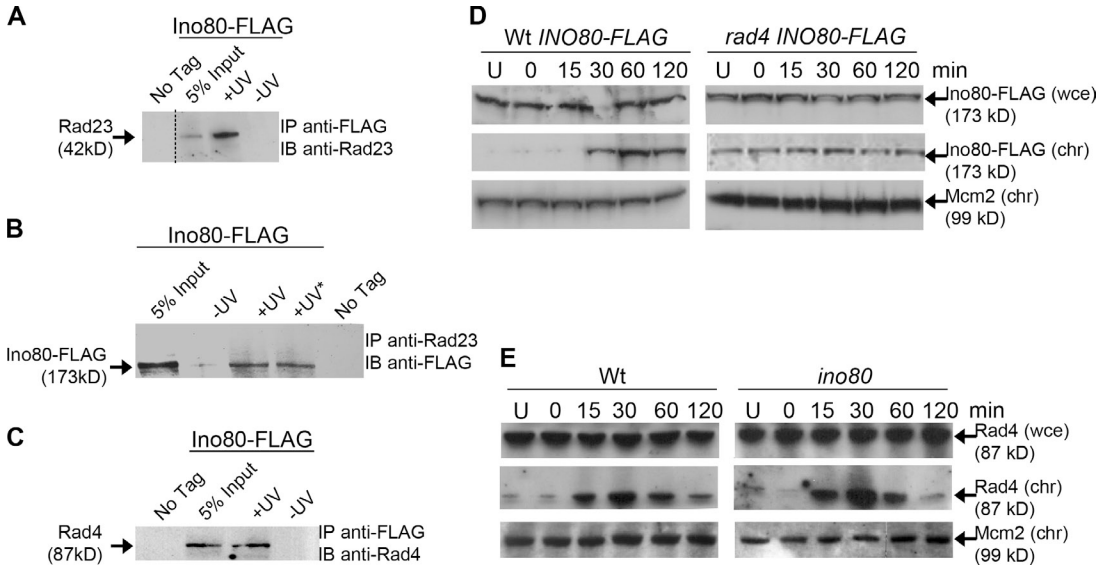

Figure 2. **UV-induced interaction of Rad23 with Ino80-FLAG.** (A) Immunoprecipitation (IP) from extracts of an Ino80-FLAG–tagged strain with anti-FLAG resin, followed by immunoblotting (IB) with anti-Rad23. Immunoprecipitations were performed either after mock-UVC treatment or irradiation with 100 J/m^2 UVC and 45-min repair. The dashed line indicates where a lane was spliced out. (B) Immunoprecipitation from extracts of an *INO80-FLAG* strain using anti-Rad23 antibodies, followed by immunoblotting with anti-FLAG. The asterisk indicates an immunoprecipitation that was subject to a high salt (0.5 M sodium chloride) wash. (C) Immunoprecipitation from extracts of an Ino80-FLAG strain with anti-FLAG resin, followed by immunoblotting with an anti-Rad4 antibody. (D) Recruitment of Ino80-FLAG to chromatin in wild-type (Wt) and *rad4* disruptants. Cells were mock treated (U) or irradiated with 100 J/m^2 UVC and incubated for up to 120 min in fresh YPD. Whole-cell extracts (wce) and chromatin fractions (chr) were isolated as described in Materials and methods. Mcm2 was used as a loading control for chromatin-bound fractions. (E) Recruitment of Rad4 to chromatin in *ino80* disruptants. Experiments were performed as in D. However, immunoblotting was performed with anti-Rad4 antibodies.

of cells with large buds after irradiation, as wild-type yeast cells arrest at late S/G2 phase after UV (Weinert and Hartwell, 1993). Wild-type and *ino80* cells exhibited an increase in budded cells within the first hour after irradiation, and both started to recover by 3 h, suggesting that *ino80* cells invoke a normal UV checkpoint and recovery response (Fig. 1 E). Consistently, phosphorylation of the checkpoint kinase Rad53 after UV irradiation occurred with similar kinetics in both wild-type and *ino80* cells (Fig. 1 F). Therefore, *ino80* cells repair UV products on a genome-wide level normally, suggesting the role of Ino80 in contributing to survival after UV repair could relate to repair in specific genomic contexts.

Ino80-C has a damage-inducible interaction with Rad4–Rad23

We next explored the molecular relationship between NER factors and Ino80. We performed reciprocal coimmunoprecipitations using chromosomally FLAG-tagged (C terminal) Ino80 with core NER factors, including Rad23, Rad14, and Rad1–Rad10. Extracts from undamaged cells and from cells treated with 100 J/m^2 UVC were examined. In one case, we could observe a robust UV-inducible interaction between Rad23 and Ino80-FLAG (Fig. 2, A and B). The interaction was identified in reciprocal experiments, immunoprecipitating with anti-FLAG and blotting with Rad23 and vice versa, and is absent in the isogenic untagged control strain (Fig. 2, A and B). The interaction between Ino80-FLAG and Rad23 is not mediated by DNA because the samples shown in Fig. 2 were all extensively treated with DNase, and the interaction is resistant to washing with buffers containing 0.5 M sodium chloride (Fig. 2 B). Rad23 has an obligate interacting partner during lesion recognition in NER, Rad4. However, Rad23 has Rad4-independent functions and is more abundant than Rad4 (Dantuma et al., 2009). We therefore asked whether Ino80 interacts with Rad4. After immunoprecipitation of Ino80-FLAG and immunoblotting for Rad4, a UV-inducible interaction between Ino80-FLAG and Rad4 was also detected (Fig. 2 C).

The damage-inducible interaction between Ino80-FLAG and Rad4–Rad23 suggests that Ino80 might be targeted to UV-damaged chromatin in a Rad4–Rad23-dependent manner. We tested this by purifying chromatin from cells after irradiation. In wild-type cells, Ino80-FLAG is recruited to chromatin after UV irradiation within 30 min (Fig. 2 D). Strikingly, in a *rad4* strain, very little chromatin recruitment of Ino80-FLAG is observed, suggesting a key role for the interaction between Ino80 and Rad4 in recruiting Ino80 to UV-damaged chromatin (Fig. 2 D). We also determined whether the association of Rad4 with damaged chromatin is perturbed in the absence of Ino80 (Fig. 2 E). Rad4 was recruited to chromatin with similar kinetics in wild-type and *ino80* cells, suggesting that Ino80 is not required for efficient damage recognition by Rad4 at a global level.

Ino80 is required for efficient UV lesion repair at *HML*α

The global repair assay in Fig. 1 C cannot reveal subtle differences in repair rates at specific genomic loci. In particular, there could be a requirement for the Ino80-C for efficient repair in genomic regions with high nucleosomal occupancy. We therefore measured the rate of photoproduct repair at two loci with very different levels of nucleosome occupancy. In our a-mating–type

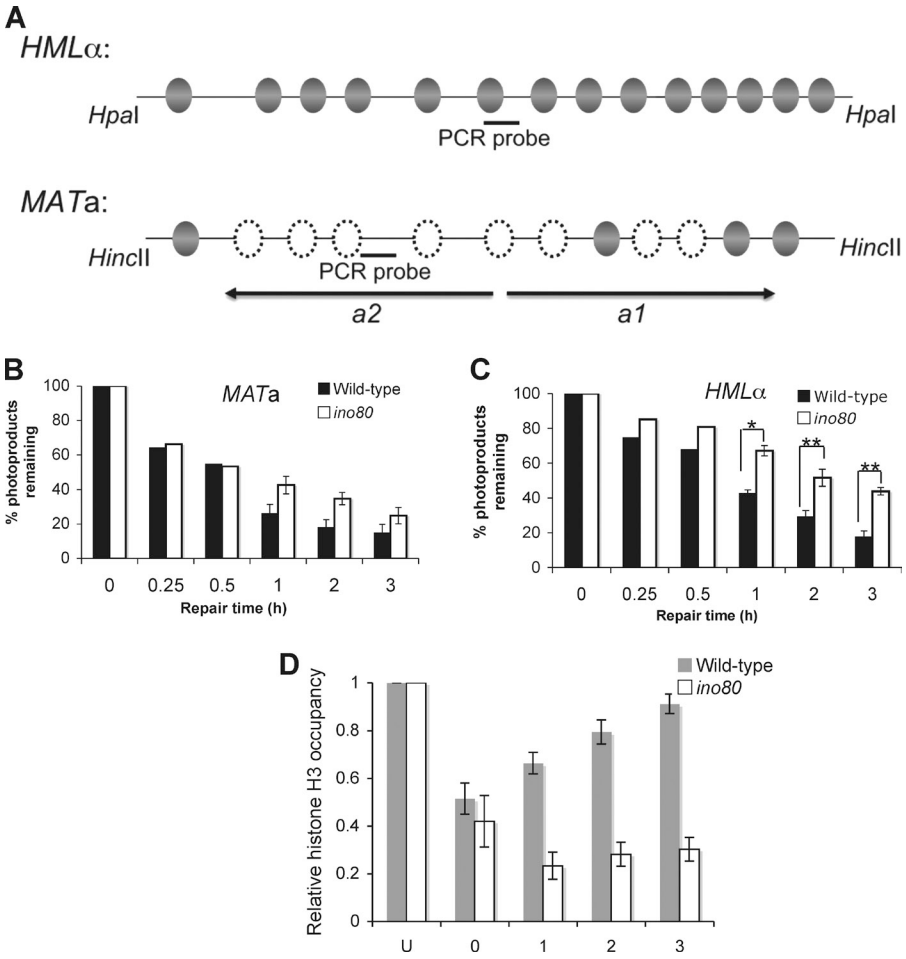

Figure 3. **Cells lacking Ino80 have defects in chromatin restoration after UV damage.** (A) Schematic representation of the *HMLα* and *MATa* loci showing the position of the defined nucleosomes relative to the PCR probes used in the repair assays at both loci and at the *HMLα* locus in the modified ChIP assay. Nucleosomes represented by broken lines are absent when the *a1* and *a2* genes of *MATa* are transcribed, as is the case in the strains used in this study. (B and C) Quantitative PCR analysis of photoproduct repair at *MATa* and *HMLα* in wild-type and *ino80* cells after 200 J/m^2 UV irradiation. For C, the single asterisk indicates $P < 0.05$, and the double asterisks indicate $P < 0.01$. (D) Analysis of histone H3 occupancy at *HMLα* before and after 200 J/m^2 UV irradiation as determined by modified ChIP in wild-type and *ino80* cells. Samples labeled U were mock irradiated. Data are the means of three repeats, and the standard deviation is shown.

strains, the *HMLα* locus is repressed, and 14 nucleosomes are bound at well-defined sites (Fig. 3 A; Weiss and Simpson, 1998). In contrast, the *MATa* locus is actively transcribed, and this is accompanied by a very low level of nucleosome occupancy (Fig. 3 A; Ravindra et al., 1999). We measured the rate of CPD removal at specific regions within *MATa* and *HMLα* (marked in Fig. 3 A) using a sensitive quantitative PCR–based assay (Fig. 3, B and C). For the chromatinized region within the *HMLα* locus, we observed that CPDs were efficiently removed over 3 h in the wild-type cells. Similar results were obtained for the nucleosome-free *MATa* locus, although repair was slightly more rapid, as expected. In *ino80* cells, repair was very slightly delayed for the *MATa* region compared with wild-type cells. Moreover, a modest but significant reduction in repair was observed in *ino80* cells at the chromatinized *HMLα* region, which was most apparent at the later time points (2 and 3 h). This suggests that Ino80 contributes to efficient repair at a chromatinized locus.

Ino80 is involved in nucleosome restoration at *HMLα* after UV

To examine chromatin dynamics at *HMLα* during UV lesion repair, we developed a novel chromatin immunoprecipitation (ChIP) methodology that permits analysis of protein occupancy at specified genomic locations in the presence of UV photoproducts (Fig. S1 A). This was necessary because UV photoproducts efficiently block the thermostable polymerases used in the PCR step of ChIP, such that fragments containing damage will be lost from analysis. In brief, after irradiation and a period of repair, cells are processed as for conventional ChIP. After immunoprecipitation and reversal of the DNA–protein cross-links, the DNA is treated with a mixture of CPD and 6-4 photoproduct photolyases and photoproducts reversed. This is essential to permit equivalent amplification of all the immunoprecipitated DNA in the sample, including fragments in which repair has yet to occur or be completed (Fig. S1, B and C).

Using this ChIP assay, we examined the nucleosomal region of *HMLα* previously analyzed in our repair experiments (Fig. 3). Antibodies recognizing the C terminus of histone H3, which bind all histone H3 present in nucleosomes regardless of their modification status or whether they also contain histone variants, were used. In a wild-type strain, histone H3 loss at a well-defined nucleosome within *HMLα* occurs almost immediately after irradiation, during the few minutes when irradiation and processing occurs, and thereafter occupancy is gradually restored over the following 3 h (Fig. 3 D). This time course is consistent with the kinetics of photoproduct repair in this strain at this locus (Fig. 3 C), where the majority of photoproducts are repaired in the first hour. ChIP performed after UV damage in cells disrupted for *ino80* indicated a similar magnitude of initial reduction in histone H3 occupancy compared with wild-type cells (Fig. 3 D). However, recovery of histone H3 occupancy

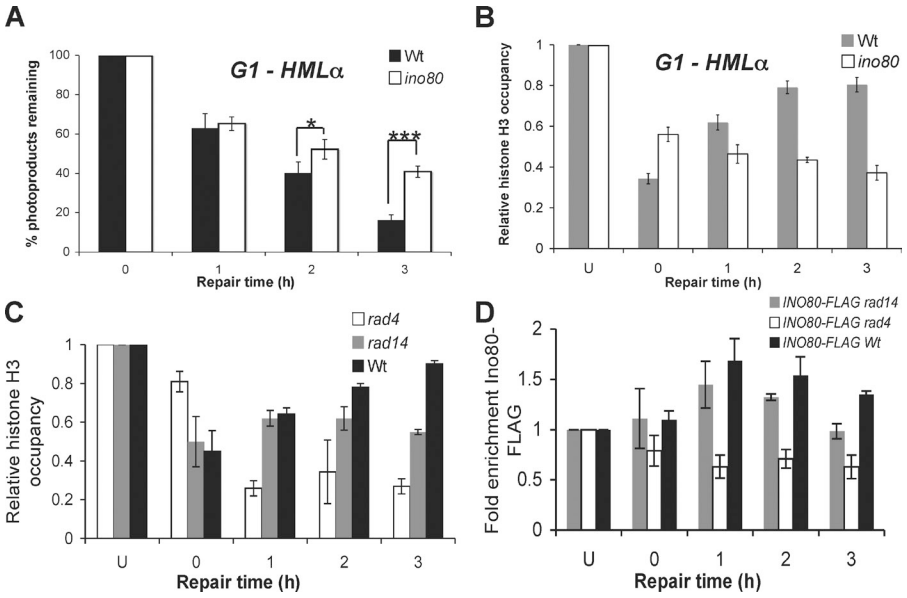

Figure 4. **Rad4 is required for rapid nucleosome remodeling at *HMLα* and the UV-induced recruitment of Ino80.** (A) Analysis of photoproduct repair at *HMLα* in wild-type (Wt) and *ino80* cells held in G1 after 200 J/m^2 UV irradiation. The single asterisk indicates $P < 0.05$, and the triple asterisk indicates $P < 0.001$ as determined by Student's *t* test. (B) ChIP of histone H3 occupancy at *HMLα* before and after 200 J/m^2 UV irradiation in wild-type and *ino80* cells held in G1. (C) Analysis of histone H3 occupancy at *HMLα* before and after 200 J/m^2 UV irradiation as determined by modified ChIP in wild-type, *rad4*, and *rad14* cells. (D) Recruitment of Ino80-FLAG to *HMLα* after UV irradiation in wild-type, *rad14*, and *rad4* cells as determined by modified ChIP. Samples labeled U were mock irradiated. Data are the means of three repeats, and the standard deviation is shown.

over the 3-h repair period is absent. This suggests that *ino80* cells have a severely impaired nucleosome restoration capacity despite only exhibiting a relatively mild repair defect at this locus. Note that the initial nucleosomal occupancy in this region of *HMLα* is equivalent for both our wild-type strain and *ino80* mutants in the undamaged state (unpublished data).

It was possible that the nucleosome loss observed after UV at *HMLα* was the result of replication fork blockage and nucleosome disassembly associated with replication-associated repair and tolerance. We therefore repeated this work in wild-type and *ino80* cells held in the G1 phase of the cell cycle with α-mating factor for the duration of treatment and recovery time. The kinetics of H3 loss at *HMLα* and the repair kinetics of lesions in this region are not significantly different from those observed in asynchronous culture (Fig. 4, A and B), indicating that the majority of the nucleosome loss we observed is a consequence of a response to UV damage that is not associated with DNA replication.

We also examined histone H3 occupancy at *HMLα* after UV treatment in *cac1* disruptants. Cac1 is a histone chaperone with a clearly established role in NER-associated chromatin restoration (Green and Almouzni, 2002). A *cac1* strain exhibited a strong decrease in H3 occupancy immediately after UV (Fig. S2 A) and exhibited little restoration of H3 signal over the following 3 h, similar to the *ino80* strain. Interestingly, however, Cac1 is not participating in the same restoration reaction as the Ino80-C during UV damage repair, as an *arp8 cac1* double mutant is not epistatic to its cognate single mutants for UV sensitivity (Fig. S2 B). Moreover, Cac1 is not required for the efficient recruitment of Ino80-FLAG to chromatin after UV damage (Fig. S2 C). This might reflect the fact that Cac1 is a histone H3 and H4 chaperone, whereas the Ino80-C has previously been shown to impact the dynamics of histone H2A and its variants, in which both might be required for efficient chromatin restoration during UV damage repair. Regardless, the defect in H3 restoration seen in the *cac1* strain is consistent with several previous studies (Mello et al., 2002; Green and Almouzni, 2003; Polo et al., 2006) and supports our assertion that we are detecting NER-associated nucleosome remodeling using the modified ChIP assay.

Rad4 is required for efficient repair-associated remodeling at *HMLα* and UV-induced recruitment of Ino80

The Rad4 (and mammalian xeroderma pigmentosum group C) protein plays a key role in initiating chromatin remodeling associated with UV repair (Baxter and Smerdon, 1998; Gong et al., 2006). Consistently, we observed an initial delay in reduction of H3 occupancy in *rad4* cells compared with the wild-type strain (Fig. 4 C), although by 1 h a reduction in histone H3 occupancy was observed. In contrast, a *rad14* strain did not exhibit any delay in initial remodeling, whereas a delay in histone restoration was apparent (Fig. 4 C). As expected, no repair was observed at *HMLα* in the course of these experiments in *rad4* or *rad14* strains (unpublished data). Therefore, damage recognition by Rad4 is needed to trigger rapid remodeling, but Rad14 is not essential to trigger this response. Moreover, NER must proceed to permit chromatin restoration because this step is eliminated in both *rad4* and *rad14* cells.

We next determined whether Ino80 is enriched at *HMLα* after UV and whether this enrichment is Rad4 dependent (Fig. 4 D). In wild-type cells, Ino80-FLAG is recruited to *HMLα*, maximally at 1 h after irradiation, and is in decline within 2–3 h. This is consistent with the Ino80-dependent histone H3 restoration kinetics observed in wild-type cells, which is near complete at 3 h after irradiation (Fig. 3 D), and also the global UV recruitment kinetics of *Ino80* (Fig. 2 D). In *rad4* cells, enrichment of Ino80-FLAG was strongly reduced after irradiation (Fig. 4 D), demonstrating that Rad4 is required to target Ino80 to *HMLα* after UV irradiation (Fig. 2 D). However, because repair is absent in *rad4* cells and repair is a prerequisite for chromatin restoration (Fig. 4 C), it could be argued that the failure to recruit Ino80-FLAG to *HMLα* is not directly a result of the absence of Rad4 but is caused by a lack of repair.

Table I. **Yeast strains used in this study**

Strain	Genotype	Source (reference)
BY4741	*MATa his3Δ1 leu2Δ0 met15Δ0 ura3Δ0*	Laboratory stock
BY4733	*MATa his3Δ200 leu2Δ0 met15Δ0 trp1Δ63 ura3Δ0*	Laboratory stock
ino80	BY4733 with *ino80::TRP1*	X. Shen (Shen et al., 2000)
INO80-2FLAG	BY4733 with *INO80-2FLAG*	X. Shen (Shen et al., 2000)
ino80 rad14	BY4733 with *ino80::TRP1 rad14::HYG*	This study
INO80-2FLAG rad4	BY4733 with *INO80-2FLAG rad4::HYG*	This study
INO80-2FLAG rad14	BY4733 with *INO80-2FLAG rad14::HYG*	This study
rad14	BY4741 with *rad14::KanMx4*	Laboratory stock
rad4	BY4741 with *rad4::KanMx4*	Laboratory stock
arp8	BY4741 with *arp::KanMX4*	Laboratory stock
arp8 cac1	BY4741 with *arp8::KanMx4 cac1::HYG*	This study
cac1	BY4741 with *cac1::HYG*	This study
INO80-2FLAG cac1	BY4733 with *INO80-2FLAG cac1::HYG*	This study

To address this, we also determined Ino80-FLAG recruitment to *HMLα* in the absence of Rad14, which is recruited after damage recognition by Rad4 and does not interact with Ino80-FLAG. In *rad14* cells, we observed robust recruitment of Ino80-FLAG to *HMLα* after UV (Fig. 4 D), despite the fact that repair is absent and chromatin restoration is defective (Fig. 4 C). Moreover, a global chromatin-binding experiment confirmed that Ino80-FLAG chromatin recruitment is efficient in *rad14* cells (Fig. S3), in contrast to *rad4* cells (Fig. 2 D). Collectively, these data show that the Rad4 damage recognition factor is required for the recruitment of Ino80-FLAG to UV-damaged chromatin regardless of whether repair by NER then proceeds.

Conclusions

Cells lacking Ino80 are UV sensitive but exhibit normal global UV photoproduct repair kinetics. Examination of a highly chromatinized region of the yeast genome, however, revealed a modest, but significant, reduction in the repair of lesions in *ino80* cells. Moreover, Ino80 interacts with Rad4–Rad23 and is recruited to chromatin after UV damage in a Rad4-dependent manner. The Ino80-C is capable of ATP-dependent nucleosome sliding, which suggests a role in nucleosome reorganization during repair. Initial experiments of a role for Ino80 in nucleosome remodeling at DSBs supported a role in nucleosome displacement (Tsukuda et al., 2005), but a recent study argued that because displacement is linked to DSB resection and because resection is delayed in *ino80* mutants, the precise role of the Ino80-C in DSB processing remains unclear (Chen et al., 2008). Our work revealed a wild type–like reduction in nucleosome occupancy at the *HMLα* after UV. Strikingly though, during repair at the *HMLα* locus, *ino80* cells fail to restore histone occupancy.

It is interesting that defective chromatin restoration is associated with a modest decrease in repair rate at this highly chromatinized locus. However, because there will be multiple repair reactions occurring within any region of DNA in close succession or simultaneously, a compromised ability to restore chromatin during the completion of NER might interfere with efficient repair within adjacent regions. In fact, there are precedents for this because defective chromatin assembly on nascent DNA (behind the replication fork) negatively impacts fork progression in S phase (Ransom et al., 2010). Moreover, although it is well established that NER is accompanied by significant changes in chromatin structure, it remains unknown whether these changes are the result of nucleosome sliding, eviction, or a combination of both (Green and Almouzni, 2002). Which is favored will profoundly affect the chromatin landscape during NER. Alternatively, it is possible that the repair defect we observe in *ino80* cells is caused by a direct role for Ino80 in facilitating the NER process itself in chromatin, unrelated to nucleosome displacement or restoration activities. However, because the repair defect at *HMLα* in *ino80* mutants is modest, but the chromatin restoration defect severe, our data clearly identify a key role for Ino80 in chromatin restoration regardless of its possible minor contribution to the core NER reaction in chromatin.

A role for the Ino80-C in nucleosomal restoration has recently been reported during promoter remodeling in response to stress (Klopf et al., 2009). Our data are also consistent with the Ino80-C playing a role in restoring chromatin structure, but in the context of NER. The contribution of the Ino80-C to this process could involve a direct role in nucleosome deposition. Alternatively, the Ino80-C might act as a nucleosome acceptor during remodeling for repair, transiently sequestering displaced nucleosomes or stabilizing remodeled nucleosomes during repair and cooperating with other assembly factors to restore chromatin structure once repair is completed. Finally, because the Ino80-C is well conserved in mammalian cells, this work has clear relevance to the human DNA damage response (Jin et al., 2005).

Materials and methods

Yeast strains and plasmids

Yeast strains are described in Table I.

Dot blot analysis of photoproduct formation and repair

The method of McCready et al. (1993) was used in this study. Antibodies against UV photoproducts used in this study were anti-CPD (Affitech) and anti–6-4 (Stratech) at a dilution of 1:1,000.

Quantitative PCR photoproduct repair assay

The quantitative PCR photoproduct repair assay was based on the method of Kalinowski et al. (1992) but with the following modifications.

Each quantitative PCR reaction contained 30 ng of genomic DNA and 10 pmol of primers: *HMLα1* (5′-TTTACTTCGAAGCCTGCT-3′), *HMLα2* (5′-ATCTTTCTTGAGTGGTCG-3′), *MATa1* (5′-AGAGGTCCGCTAATTCTG-3′), *MATa2* (5′-CTTACAGAGGACACCGGT-3′), and SensiMix from the SYBR kit (Bioline). Samples were analyzed on the Research Rotor Gene 3000 (Corbett Life Science).

Coimmunoprecipitations

Strains with chromosomally FLAG-tagged *INO80* were grown to logarithmic phase, UV damaged with 100 J/m^2 UVC or mock irradiated, and allowed to repair for 45 min in rich media (YEPD [yeast extract, peptone, dextrose]). Whole-cell extracts were then immunoprecipitated with anti-Rad23, and protein was analyzed on 4–12% Bis-Tris Gels (Invitrogen) blotted with an anti-FLAG mouse polyclonal antibody (1:1,000 dilution; Abcam). FLAG immunoprecipitations were performed using M2 anti-FLAG resin (Sigma-Aldrich), and elution was performed with 3× anti-FLAG peptide (Sigma-Aldrich). Gels were immunoblotted with polyclonal anti-Rad23 (1:1,000) or anti-Rad4 (1:5,000). Where DNase I treatment was used, extracts were treated with 5 U for 1 h at 37°C.

Chromatin-binding assays

Chromatin-binding assays were performed essentially as described previously (Liang and Stillman, 1997). In brief, 10^9 cells were harvested, spheroplasted using Zymolase 20T at 30°C for 15 min, and then lysed in 100 mM KCl, 50 mM Hepes-KOH, pH 7.5, 2.5 mM $MgCl_2$, 50 mM NaF, 0.25% of final volume Triton X-100 supplemented with protease inhibitor tablets (Roche), and 1 mM PMSF. Chromatin, nuclear matrix, and cell debris were spun down at 4,000 rpm for 5 min. The crude pellet was treated with 0.6 U of limited micrococcal nuclease digestion in the aforementioned buffer for 3 min at 37°C and spun down at 4,000 rpm for 10 min. The solubilized polynucleosomes were then pelleted at high speed (50,000 rpm) for 1 h at 4°C.

Modified ChIP

Formaldehyde (TAAB Laboratories) was added to cells to a final concentration of 1%, and incubation for 30 min at room temperature followed. Glycine was added to a final concentration of 125 mM, and cells were incubated for 5 min. Cell pellets were resuspended in lysis buffer (50 mM Hepes-NaOH, pH 7.5, 140 mM NaCl, 1 mM EDTA, 1% Triton X-100, and 0.1% sodium deoxycholate) containing protease inhibitor solution (Complete; Roche) and 1 mM PMSF together with acid-washed glass beads and cells lysed using a bead beater. Debris was removed by centrifugation for 5 min at 2,000 rpm. Chromatin was sheared by sonication at 40% output for 5 s eight times before the lysate was clarified by centrifugation and twice at 13,000 rpm for 20 min. 2 µg antihistone H3 ChIP-grade antibody (Abcam) was added to 500 µg of protein extract and rotated overnight at 4°C. Cell extracts were also frozen for processing as input controls. 40 µl of 50% slurry protein G Sepharose was added to the protein–antibody mixture and rotated for 1 h. The beads were collected by centrifugation at 13,000 rpm for 15 s and washed with 1.5 ml of lysis buffer. The beads were washed again with 1.5 ml of lysis buffer containing 500 mM NaCl followed by 1.5 ml radioimmunoprecipitation assay and 1.5 ml TE (Tris-EDTA), pH 8.0. The beads were resuspended in 100 µl TE, pH 8.0, and incubated with 20 µg RNase A (Sigma-Aldrich) for 30 min at 37°C. 1 ml TE, pH 8.0, was added, and beads were collected by centrifugation. Protein–DNA complexes were eluted by incubating twice with 250 µl of elution buffer (1% SDS and 0.1-M $NaHCO_3$). 20 µl of 5-M NaCl was added to the eluate and input samples, which were incubated overnight at 65°C. 1 ml ethanol was added to each sample, and samples were incubated overnight at −20°C before being centrifuged for 15 min at 13,000 rpm at 4°C. The pellet was washed with 70% ethanol, resuspended in 100 µl TE, pH 8.0, and treated with 20 µg proteinase K at 50°C for 30 min. The DNA was extracted once with phenol:chloroform:isoamyl alcohol followed by extraction of the organic phase with TE. The DNA was precipitated and then resuspended in 50 µl of TE, pH 8.0. 50 µl of extracted DNA was incubated with reactivation buffer (20 mM Tris-HCl, pH 7.8, 50 mM NaCl, 1 mM EDTA, and 1 mM DTT [Sigma-Aldrich]), 5 mM DTT, 5 µg *D. melanogaster* 6-4 photolyase (purified according to Kim et al., 1994; a gift from A. Sancar, University of North Carolina at Chapel Hill, Chapel Hill, NC), and 50 ng *Escherichia coli* CPD photolyase (R&D Systems). The reactions were incubated under a blacklight bulb and conventional lightbulb for the 6-4 and CPD enzymes, respectively, for 1 h at room temperature. After incubation, the reactions were purified using a purification kit (QIAquick PCR; QIAGEN). The column was eluted using 100 µl of deionized H_2O. Quantitative PCR reactions contained 13 µl of SensiMix SYBR kit, 10 pmol of the forward and reverse primers (sequences as used in the Quantitative PCR photoproduct repair assay section at *HMLα*), 5 µl of immunoprecipitated DNA, and 5 µl of 0.02-ng pUC19. Reactions were performed on the Research Rotor Gene 3000, once using mastermix containing primers to specific regions of *HMLα* and once using M13 primers to pUC19. Threshold cycle values for immunoprecipitated DNA were normalized to both input and no antibody controls.

Immunoblots and protein analysis

The anti-Rad4 antibody was a gift from S. Reed (Cardiff University, Cardiff, Wales, UK) and was used at a dilution of 1:5,000. Polyclonal anti-Rad10, anti-Rad23, and anti-Rad53 antibodies were obtained from Santa Cruz Biotechnology, Inc., and anti-Rad14 was obtained from Abcam. Each was used at a dilution of 1:1,000.

Online supplemental material

Fig. S1 illustrates the modified ChIP assay schematically and the reasons for its development. Fig. S2 confirms that Cac1 is required for chromatin restoration after UV damage but probably contributes to a different reaction than Ino80. Fig. S3 shows that Rad14 is not required for Ino80-FLAG recruitment to UV-damaged chromatin. Online supplemental material is available at http://www.jcb.org/cgi/content/full/jcb.201006178/DC1.

We are grateful to Ian Hickson and Leonard Wu for helpful comments on the manuscript. We thank Simon Reed, Xuetong Shen (University of Texas MD Anderson Cancer Center, Smithville, TX), and Aziz Sancar for sharing yeast strains, plasmids, and antibodies.

This work was supported by Cancer Research UK.

Submitted: 29 June 2010
Accepted: 9 November 2010

References

Aboussekhra, A., M. Biggerstaff, M.K. Shivji, J.A. Vilpo, V. Moncollin, V.N. Podust, M. Protić, U. Hübscher, J.M. Egly, and R.D. Wood. 1995. Mammalian DNA nucleotide excision repair reconstituted with purified protein components. *Cell.* 80:859–868. doi:10.1016/0092-8674(95)90289-9

Baxter, B.K., and M.J. Smerdon. 1998. Nucleosome unfolding during DNA repair in normal and xeroderma pigmentosum (group C) human cells. *J. Biol. Chem.* 273:17517–17524. doi:10.1074/jbc.273.28.17517

Chen, C.C., J.J. Carson, J. Feser, B. Tamburini, S. Zabaronick, J. Linger, and J.K. Tyler. 2008. Acetylated lysine 56 on histone H3 drives chromatin assembly after repair and signals for the completion of repair. *Cell.* 134:231–243. doi:10.1016/j.cell.2008.06.035

Dantuma, N.P., C. Heinen, and D. Hoogstraten. 2009. The ubiquitin receptor Rad23: at the crossroads of nucleotide excision repair and proteasomal degradation. *DNA Repair (Amst.).* 8:449–460. doi:10.1016/j.dnarep.2009.01.005

Dinant, C., A.B. Houtsmuller, and W. Vermeulen. 2008. Chromatin structure and DNA damage repair. *Epigenetics Chromatin.* 1:9. doi:10.1186/1756-8935-1-9

Downs, J.A., S. Allard, O. Jobin-Robitaille, A. Javaheri, A. Auger, N. Bouchard, S.J. Kron, S.P. Jackson, and J. Côté. 2004. Binding of chromatin-modifying activities to phosphorylated histone H2A at DNA damage sites. *Mol. Cell.* 16:979–990. doi:10.1016/j.molcel.2004.12.003

Downs, J.A., M.C. Nussenzweig, and A. Nussenzweig. 2007. Chromatin dynamics and the preservation of genetic information. *Nature.* 447:951–958. doi:10.1038/nature05980

Falbo, K.B., C. Alabert, Y. Katou, S. Wu, J. Han, T. Wehr, J. Xiao, X. He, Z. Zhang, Y. Shi, et al. 2009. Involvement of a chromatin remodeling complex in damage tolerance during DNA replication. *Nat. Struct. Mol. Biol.* 16:1167–1172. doi:10.1038/nsmb.1686

Gong, F., D. Fahy, and M.J. Smerdon. 2006. Rad4-Rad23 interaction with SWI/SNF links ATP-dependent chromatin remodeling with nucleotide excision repair. *Nat. Struct. Mol. Biol.* 13:902–907. doi:10.1038/nsmb1152

Green, C.M., and G. Almouzni. 2002. When repair meets chromatin. First in series on chromatin dynamics. *EMBO Rep.* 3:28–33. doi:10.1093/embo-reports/kvf005

Green, C.M., and G. Almouzni. 2003. Local action of the chromatin assembly factor CAF-1 at sites of nucleotide excision repair in vivo. *EMBO J.* 22:5163–5174. doi:10.1093/emboj/cdg478

Guzder, S.N., Y. Habraken, P. Sung, L. Prakash, and S. Prakash. 1995. Reconstitution of yeast nucleotide excision repair with purified Rad

proteins, replication protein A, and transcription factor TFIIH. *J. Biol. Chem.* 270:12973–12976. doi:10.1074/jbc.270.22.12973

Hara, R., and A. Sancar. 2003. Effect of damage type on stimulation of human excision nuclease by SWI/SNF chromatin remodeling factor. *Mol. Cell. Biol.* 23:4121–4125. doi:10.1128/MCB.23.12.4121-4125.2003

Jin, J., Y. Cai, T. Yao, A.J. Gottschalk, L. Florens, S.K. Swanson, J.L. Gutiérrez, M.K. Coleman, J.L. Workman, A. Mushegian, et al. 2005. A mammalian chromatin remodeling complex with similarities to the yeast INO80 complex. *J. Biol. Chem.* 280:41207–41212. doi:10.1074/jbc.M509128200

Kalinowski, D.P., S. Illenye, and B. Van Houten. 1992. Analysis of DNA damage and repair in murine leukemia L1210 cells using a quantitative polymerase chain reaction assay. *Nucleic Acids Res.* 20:3485–3494. doi:10.1093/nar/20.13.3485

Kim, S.T., K. Malhotra, C.A. Smith, J.S. Taylor, and A. Sancar. 1994. Characterization of (6-4) photoproduct DNA photolyase. *J. Biol. Chem.* 269:8535–8540.

Klopf, E., L. Paskova, C. Solé, G. Mas, A. Petryshyn, F. Posas, U. Wintersberger, G. Ammerer, and C. Schüller. 2009. Cooperation between the INO80 complex and histone chaperones determines adaptation of stress gene transcription in the yeast *Saccharomyces cerevisiae*. *Mol. Cell. Biol.* 29:4994–5007. doi:10.1128/MCB.01858-08

Liang, C., and B. Stillman. 1997. Persistent initiation of DNA replication and chromatin-bound MCM proteins during the cell cycle in cdc6 mutants. *Genes Dev.* 11:3375–3386. doi:10.1101/gad.11.24.3375

McCready, S., A.M. Carr, and A.R. Lehmann. 1993. Repair of cyclobutane pyrimidine dimers and 6-4 photoproducts in the fission yeast *Schizosaccharomyces pombe*. *Mol. Microbiol.* 10:885–890. doi:10.1111/j.1365-2958.1993.tb00959.x

Mello, J.A., H.H. Silljé, D.M. Roche, D.B. Kirschner, E.A. Nigg, and G. Almouzni. 2002. Human Asf1 and CAF-1 interact and synergize in a repair-coupled nucleosome assembly pathway. *EMBO Rep.* 3:329–334. doi:10.1093/embo-reports/kvf068

Morrison, A.J., J. Highland, N.J. Krogan, A. Arbel-Eden, J.F. Greenblatt, J.E. Haber, and X. Shen. 2004. INO80 and gamma-H2AX interaction links ATP-dependent chromatin remodeling to DNA damage repair. *Cell.* 119:767–775. doi:10.1016/j.cell.2004.11.037

Mu, D., C.H. Park, T. Matsunaga, D.S. Hsu, J.T. Reardon, and A. Sancar. 1995. Reconstitution of human DNA repair excision nuclease in a highly defined system. *J. Biol. Chem.* 270:2415–2418. doi:10.1074/jbc.270.6.2415

Osley, M.A., T. Tsukuda, and J.A. Nickoloff. 2007. ATP-dependent chromatin remodeling factors and DNA damage repair. *Mutat. Res.* 618:65–80.

Papamichos-Chronakis, M., and C.L. Peterson. 2008. The Ino80 chromatin-remodeling enzyme regulates replisome function and stability. *Nat. Struct. Mol. Biol.* 15:338–345. doi:10.1038/nsmb.1413

Polo, S.E., D. Roche, and G. Almouzni. 2006. New histone incorporation marks sites of UV repair in human cells. *Cell.* 127:481–493. doi:10.1016/j.cell.2006.08.049

Ransom, M., B.K. Dennehey, and J.K. Tyler. 2010. Chaperoning histones during DNA replication and repair. *Cell.* 140:183–195. doi:10.1016/j.cell.2010.01.004

Ravindra, A., K. Weiss, and R.T. Simpson. 1999. High-resolution structural analysis of chromatin at specific loci: *Saccharomyces cerevisiae* silent mating-type locus HMRa. *Mol. Cell. Biol.* 19:7944–7950.

Riedl, T., F. Hanaoka, and J.M. Egly. 2003. The comings and goings of nucleotide excision repair factors on damaged DNA. *EMBO J.* 22:5293–5303. doi:10.1093/emboj/cdg489

Shen, X., G. Mizuguchi, A. Hamiche, and C. Wu. 2000. A chromatin remodelling complex involved in transcription and DNA processing. *Nature.* 406:541–544. doi:10.1038/35020123

Shimada, K., Y. Oma, T. Schleker, K. Kugou, K. Ohta, M. Harata, and S.M. Gasser. 2008. Ino80 chromatin remodeling complex promotes recovery of stalled replication forks. *Curr. Biol.* 18:566–575. doi:10.1016/j.cub.2008.03.049

Smerdon, M.J. 1991. DNA repair and the role of chromatin structure. *Curr. Opin. Cell Biol.* 3:422–428. doi:10.1016/0955-0674(91)90069-B

Staresincic, L., A.F. Fagbemi, J.H. Enzlin, A.M. Gourdin, N. Wijgers, I. Dunand-Sauthier, G. Giglia-Mari, S.G. Clarkson, W. Vermeulen, and O.D. Schärer. 2009. Coordination of dual incision and repair synthesis in human nucleotide excision repair. *EMBO J.* 28:1111–1120. doi:10.1038/emboj.2009.49

Teng, Y., H. Liu, H.W. Gill, Y. Yu, R. Waters, and S.H. Reed. 2008. *Saccharomyces cerevisiae* Rad16 mediates ultraviolet-dependent histone H3 acetylation required for efficient global genome nucleotide-excision repair. *EMBO Rep.* 9:97–102. doi:10.1038/sj.embor.7401112

Tsukuda, T., A.B. Fleming, J.A. Nickoloff, and M.A. Osley. 2005. Chromatin remodelling at a DNA double-strand break site in *Saccharomyces cerevisiae*. *Nature.* 438:379–383. doi:10.1038/nature04148

Ura, K., M. Araki, H. Saeki, C. Masutani, T. Ito, S. Iwai, T. Mizukoshi, Y. Kaneda, and F. Hanaoka. 2001. ATP-dependent chromatin remodeling facilitates nucleotide excision repair of UV-induced DNA lesions in synthetic dinucleosomes. *EMBO J.* 20:2004–2014. doi:10.1093/emboj/20.8.2004

van Attikum, H., and S.M. Gasser. 2009. Crosstalk between histone modifications during the DNA damage response. *Trends Cell Biol.* 19:207–217. doi:10.1016/j.tcb.2009.03.001

van Attikum, H., O. Fritsch, B. Hohn, and S.M. Gasser. 2004. Recruitment of the INO80 complex by H2A phosphorylation links ATP-dependent chromatin remodeling with DNA double-strand break repair. *Cell.* 119:777–788. doi:10.1016/j.cell.2004.11.033

van Attikum, H., O. Fritsch, and S.M. Gasser. 2007. Distinct roles for SWR1 and INO80 chromatin remodeling complexes at chromosomal double-strand breaks. *EMBO J.* 26:4113–4125. doi:10.1038/sj.emboj.7601835

Wang, H., L. Zhai, J. Xu, H.Y. Joo, S. Jackson, H. Erdjument-Bromage, P. Tempst, Y. Xiong, and Y. Zhang. 2006. Histone H3 and H4 ubiquitylation by the CUL4-DDB-ROC1 ubiquitin ligase facilitates cellular response to DNA damage. *Mol. Cell.* 22:383–394. doi:10.1016/j.molcel.2006.03.035

Weinert, T.A., and L.H. Hartwell. 1993. Cell cycle arrest of cdc mutants and specificity of the RAD9 checkpoint. *Genetics.* 134:63–80.

Weiss, K., and R.T. Simpson. 1998. High-resolution structural analysis of chromatin at specific loci: *Saccharomyces cerevisiae* silent mating type locus HMLalpha. *Mol. Cell. Biol.* 18:5392–5403.